

# Large Variations in Single Molecule Conductance of Cyclic and Bicyclic Silanes

Haixing Li,<sup>‡1</sup> Marc H. Garner,<sup>‡2</sup> Zhichun Shangguan,<sup>‡3</sup> Yan Chen,<sup>3</sup> Qianwen Zheng,<sup>3</sup> Timothy Su,<sup>4</sup> Madhav Neupane,<sup>4</sup> Taifeng Liu,<sup>3</sup> Michael Steigerwald,<sup>4</sup> Fay Ng,<sup>4</sup> Colin Nuckolls,<sup>4</sup> Shengxiong Xiao,<sup>\*3</sup> Gemma Solomon,<sup>\*2</sup> Latha Venkataraman,<sup>\*1,4</sup>

<sup>1</sup>Department of Applied Physics and Applied Mathematics, Columbia University, New York, New York 10027, United States

<sup>2</sup>Nano-Science Center and Department of Chemistry, University of Copenhagen, Universitetsparken 5, 2100 Copenhagen Ø, Denmark

<sup>3</sup>The Education Ministry Key Lab of Resource Chemistry, Shanghai Key Laboratory of Rare Earth Functional Materials, Optoelectronic Nano Materials and Devices Institute, Department of Chemistry, Shanghai Normal University, Shanghai 200234, China

<sup>4</sup>Department of Chemistry, Columbia University, New York, New York 10027, United States

## Supporting Information Placeholder

**ABSTRACT:** Linear silanes are efficient molecular wires due to strong  $\sigma$ -conjugation in the transoid conformation, however, the structure-function relationship for the conformational dependence of single-molecule conductance of silanes remains untested. Here we report the syntheses, electrical measurements, and theoretical characterization of four series of functionalized cyclic and bicyclic silanes including a cyclotetrasilane, a cyclopentasilane, a bicyclo[2.2.1]heptasilane, and a bicyclo[2.2.2]octasilane, which are all extended by linear silicon linkers of varying length. We find an unusual variation of the single-molecule conductance between the four series at each linker-length. We determine the relative conductance of the (bi)cyclic silicon structures by using the common length dependence of the four series rather than comparing the conductance at a single length. Contrasting with the cyclic  $\pi$ -conjugated molecules, the conductance of  $\sigma$ -conjugated (bi)cyclic silanes is dominated by a single path through the molecule and is controlled by the dihedral angles along this path. This strong sensitivity to molecular conformation dictates the single-molecule conductance of  $\sigma$ -conjugated silanes and allows for systematic control of the conductance through molecular design.

## INTRODUCTION

With a continuing miniaturization of silicon devices,<sup>1</sup> molecules consisting of several silicon atoms become ideal systems to understand nanoscale transport in silicon. The continued progress in silane synthesis<sup>2-9</sup> has opened up a whole range of molecular topologies and revealed the rich complexity of electronic communication through silanes.

Linear silicon-based chains can be highly conducting and sensitive to conformation as molecular silanes<sup>10</sup> or alternatively extremely insulating if they are modified to molecular siloxane.<sup>11</sup> Cyclic and bicyclic silicon ring structures further influence the

electron-transport properties, not the least of which from the significant conformational flexibility that some cyclic structures possess.<sup>12</sup> Furthermore, as can be used to test the theoretical prediction about different superposition regimes in parallel molecular wires<sup>13</sup>, highly constrained silane systems with multiple pathways were used to demonstrate that different bridges do not act as parallel resistors.<sup>14-15</sup>

$\sigma$ -conjugation in silanes and alkanes depends on the dihedral angles in the molecular backbone;<sup>16-19</sup> and single-molecule conductance is expected to reflect this dependence.<sup>20-22</sup> For example, we recently found that there is destructive quantum interference in the bicyclo[2.2.2]octasilane molecular unit due to its constrained dihedral angles; consequently the conductance is effectively suppressed.<sup>23</sup> It is clear that in between the high conductance all-*transoid* linear silanes and low conductance bicyclic silanes with *cisoid* dihedral angles, there is a range of accessible silane systems with a variation of backbone dihedral angles.<sup>24</sup> Experimental studies, however, have been somewhat limited to exploring photophysical properties<sup>25-28</sup> and the relationship between backbone dihedrals and charge carrier mobility in conducting silane polymers.<sup>29-31</sup>

In this work we investigate how best to gain broad insight into the transport properties of linear, cyclic and bicyclic silanes when these properties are very sensitive to conformation and conformational flexibility varies significantly across different structures. In addition to the linear silanes that have been studied previously, we employ a series of molecules designed and synthesized for this purpose, as displayed in Figure 1a: cyclotetrasilane (**4-ring**), cyclopentasilane (**5-ring**), bicyclo[2.2.1]heptasilane (**221**), and bicyclo[2.2.2]octasilane (**222**). These basic structures are expanded to a family of molecules by extending the backbone length. Here, we investigate their single-molecule conductance properties using the scanning tunneling microscope break junction (STM-BJ) technique as well as density functional theory (DFT) transport calculations.

This paper proceeds as follows. We employ a simple method to determine the relative conductance of the silicon ring units, disregarding the variable conformational flexibility in the molecules. This is achieved by fitting the conductance values of the molecules at all lengths and extrapolating the fit to zero length, similar to that previously employed for finding contact resistance and the resistance of a repeat unit in extended systems.<sup>32-33</sup> This method relies on the fact that linear silanes show a clear exponential attenuation of conductance with increasing length.<sup>10</sup> These trends are expected to be general when contact geometries and conformations of the linear wire do not vary significantly. Using this approach, we establish the structure-function relationship and find a conductance trend of  $G_{221} > G_{4\text{-ring}} > G_{5\text{-ring}} > G_{222}$ . We are then able to gain insight into the transport properties of the silanes more generally and specifically probe the roles of multiple paths, dihedral angles, and  $\sigma$ -interference.

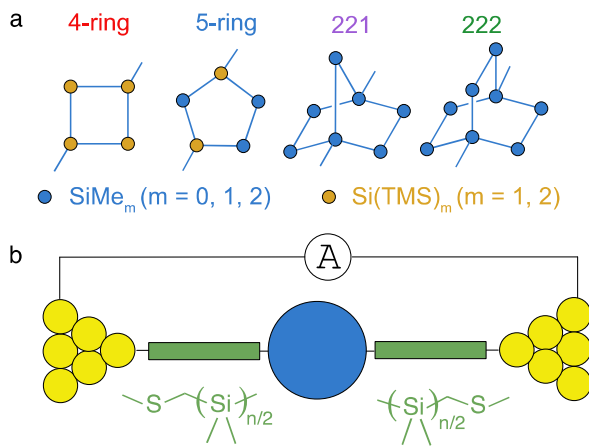


Figure 1. (a) Chemical structures of the central subunits. The two dangling bonds on each structure indicate the positions for attaching the linear silicon wires. The extending silicon chain length is:  $n = 2, 4, 6$  for **4-ring** and **5-ring** and  $n = 0, 2, 4, 6$  for **221** and **222**. TMS represents a trimethylsilyl group and Me a methyl group. (b) Schematic of a single molecule junction formed with a silicon molecular wire containing a ring (blue dot) and extending arm (green rectangles).

## METHODS

### The Molecular Systems

To compare the single-molecule junction conductance of the four silicon ring units, we synthetically attach silicon molecular wires to these systems and create a series of molecules with different chain lengths with  $n = 2, 4, 6$  for **4-ring** and **5-ring**;  $n = 0, 2, 4, 6$  for **221** and **222**. The **4-ring** and **5-ring** have cis and trans isomers; here we focus on the trans isomers; results comparing cis and trans isomers have been detailed previously.<sup>12</sup> The synthetic details are described in the supporting information (SI Part IV).<sup>10, 34-38</sup> Each silicon arm is functionalized with terminal methylthiolmethyl groups to enable the formation of molecular junctions with Au electrodes.<sup>34</sup>

### Single Molecule Conductance Measurements

We measure the conductance of single-molecule junctions using a STM-BJ method (Figure 1b).<sup>39-40</sup> For each molecule, we repeatedly form and break Au point contacts in a 1,2,4-trichlorobenzene solution of the target molecule. The conductance

versus displacement traces reveal plateaus near integer multiples of the conductance quantum ( $G_0, 2e^2/h$ ) with one or sometimes two additional plateaus below  $G_0$ ; these additional steps indicate the formation of Au-molecule-Au junctions.

We compile 10,000 – 30,000 traces into a logarithmically-binned conductance histogram for each molecule studied without any data selection. Figure 2a-d display the conductance histograms for the **222**, **221**, **4-ring** and **5-ring** series with different chain lengths. We see clear conductance peaks for all systems, indicating that the silicon ring structures provide an electronic pathway and are well-coupled in the junction. Here we focus on the most significant peak for each molecule.<sup>12</sup> We obtain the most probable conductance value for each molecule by fitting a Gaussian function to the conductance peak that corresponds to a fully elongated junction as determined from 2-dimensional histograms (Figure S1 – S4).

### Density Functional Theory Calculations

To investigate the nature of the transport through these silicon ring structures, we perform *ab initio* calculations based on density functional theory (DFT). The molecular structures are optimized in vacuum and placed between two 4-atom Au-pyramids on  $5 \times 5$  fcc Au(111) surfaces to form a junction. The molecule is relaxed to a threshold of 0.05 eV/Å with the Au-atoms kept fixed. DFT with the PBE exchange-correlation functional, double- $\zeta$  plus polarization basis set for the molecule, and double- $\zeta$  basis set for the Au atoms are used as implemented in ASE and GPAW.<sup>41-44</sup> The optimized junction structures are transferred to  $6 \times 6$  fcc Au(111) surfaces and the transmission is calculated with the non-equilibrium Green's function approach as implemented in Virtual NanoLab and Atomistix ToolKit.<sup>45-48</sup>

We calculate the interatomic transmission pathways at the Fermi energy as described in detail elsewhere.<sup>21</sup> The transmission contributions between atoms are plotted as arrows on top of the optimized junction structures, where the cross-sectional area of each arrow scales proportionally with the interatomic transmission. Arrows in the transport direction are colored in red, arrows opposite the transport direction in blue. For clarity a threshold of 10% of the total transmission is applied; smaller arrows are not shown. A more detailed description of the theoretical procedure and all transmission plots are included in SI Part III.

## RESULTS

In Figure 2e, we plot the single-molecule junction conductance as a function of the number of silicon atoms in the silane arms. These data reveal that the conductance decreases exponentially with increasing length,  $G = G_0 e^{-\beta n}$ , except for the **222** series. We find that **4-ring**, **5-ring** and **221** series share a very similar tunneling decay constant  $\beta$  (Table 1) determined from the fit to the conductance data with  $\beta = 0.73-0.82$  per silicon, which is close to that of linear silanes at  $\beta = 0.75$  per silicon (or  $0.39 \text{ \AA}^{-1}$ ).<sup>10</sup>

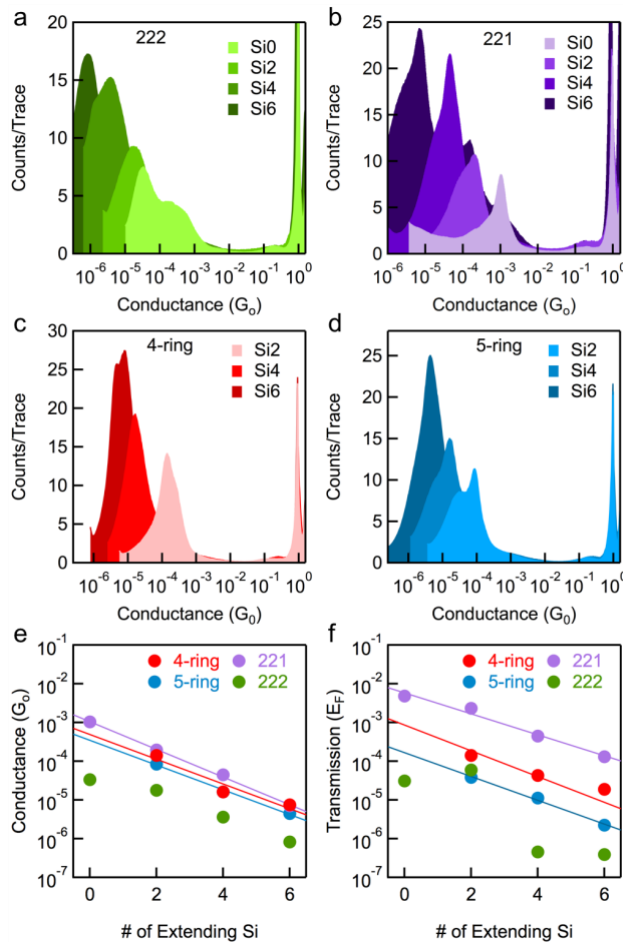


Figure 2. Conductance histograms for silicon molecular wires containing (a) 222, (b) 221, (c) 4-ring and (d) 5-ring. The counts/trace intensity of the 221(Si6) data is multiplied by a factor of 3. The number of silicon atoms in the oligosilane wire  $[SiMe_2]_n$  ( $n = 0, 2, 4, 6$ ) is indicated by a light to dark color scheme. (e) Measured single-molecule junction conductance and (f) calculated transmissions at the Fermi energy plotted against silane arm

Table 1. Relative Conductance and Decay Constants of the 221, 4-ring, 5-ring and 222 systems determined from STM-BJ measurements and DFT calculations.

Molecule	Measured <sup>a</sup>					Calculated	Measured	Calculated
	$G_{Si0}/G_L$ <sup>b</sup>	$G_{Si2}/G_L$	$G_{Si4}/G_L$	$G_{Si6}/G_L$	$G_{n=0}/G_L$ <sup>c</sup>			
221	1.10	0.97	1.01	0.74	1.12	0.92	$0.82 \pm 0.03$	$0.62 \pm 0.06$
4-ring	NA	0.71	0.36	0.79	0.52	0.17	$0.73 \pm 0.20$	$0.50 \pm 0.05$
5-ring	NA	0.42	0.36	0.47	0.37	0.03	$0.73 \pm 0.06$	$0.71 \pm 0.05$
222	0.09	0.21	0.15	0.18	NA	NA	NA	NA

<sup>a</sup> Conductance peak values are obtained from fitting a Gaussian function to the corresponding 1D conductance histogram. <sup>b</sup> To calculate each conductance ratio, we divide the conductance of the indicated silicon-ring wire to its corresponding linear counterpart. The linear counterparts are Si3, Si5, Si7 and Si9 for 221, 4-ring and 5-ring; are Si4, Si6, Si8, and Si10 for 222. <sup>c</sup> Ring conductance determined from the intersect of the fit at  $n = 0$ .

### Variability Across the Series: Odd-Even Effect

## DISCUSSION

length for 221 (purple), 4-ring (red), 5-ring (blue), 222 (green) based oligosilanes. Lines show linear fits to the data following  $G = G_0 e^{-\beta n}$ .

We find that the relative conductance between the ring structures can vary significantly depending on the molecular length. This result strongly suggests that we cannot simply compare the four ring structures at one particular length but need to consider a series of lengths and extrapolate the effective conductance  $G_c$  at  $n = 0$ , as listed in Table 1. Applying this method, we can conclude that **5-ring** is a worse conductor than **4-ring**, a result that is not so clear at each fixed length. In addition, we observe an odd-even effect in the conductance of the **4-ring** series as can be seen in Figure 2. This phenomenon is intrinsic to **4-ring** systems as we also observe the odd-even effect in three other series containing **4-ring**. (SI Figure S5, S6)

The transmission calculated at the Fermi energy is plotted against the chain length for each series in Figure 2f. We find this calculated conductance captures the trend  $G_{221} > G_{4\text{-ring}} > G_{5\text{-ring}} > G_{222}$  shown in experimental data in Figure 2e and Table 1. While some of the experimental conductance features, including the odd-even alternation of the **4-ring** systems, are qualitatively reproduced by the calculations, we note the exact transmission values lack quantitative accuracy. As we explore in more detail in SI part III, we find that particularly in systems where the transmission is sensitive to the Fermi energy alignment, the transmission at the Fermi energy does not reproduce the experimental conductance. As has been discussed in other reports, the quantitative mismatch between theory and experiment is to be expected due to errors inherent to DFT.<sup>12, 49-51</sup>

We find the calculated decay constant for the **5-ring** and linear silane systems agree with the experimental data. For **4-ring** and **221**, the experimental decay constant is larger than the calculated value. Specifically, for **4-ring**, the transmission at the Fermi energy is very sensitive to the Fermi energy alignment as shown in Figure S11. Despite the discrepancy between experiment and calculations for **221**, its calculated decay constant and transmission values are very similar to those of linear silanes (Figure S13).

From the measured conductance in Figure 2e and Table 1, there is a notable *odd-even* conductance fluctuation with length in the **4-ring** series, and to some extent also in the **222** series, that limits the value in comparing the conductance of different (bi)cyclic structures at any one length. In order to understand the origin of this effect, we show the tip-to-tip Au-Au length of the calculated single-molecule junctions of the **4-ring** series in Figure 3 together with ball and stick models of the molecules at their fully extended structures. These calculations represent a junction geometry right before the S-Au contact breaks. From the junction structures, we notice that there is a clear odd-even alternation in the junction lengths for the **4-ring** series. Due to the constrained bond angles of the cyclic system, the zig-zag pattern of the transoid conformation in linear silane arms gives rise to alternating junction lengths. The same structural pattern can be seen for the **222** series in Figure S23. This suggests the following correlation: the Si0 and Si4 extended systems are *long* and may therefore have lower transmission probability than the general trend for the series; conversely, the Si2 and Si6 extended systems are *short* and may have a higher transmission than the general trend suggests.

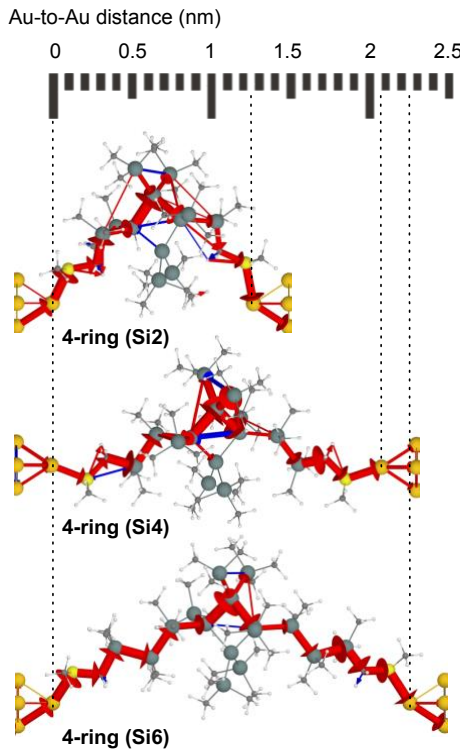


Figure 3. Optimized junction structure and interatomic transmission pathway analysis of **4-ring** series. The calculated tip Au-Au junction length is illustrated with the nanometer-ruler on the top.

In Figure 4, we compare the calculated and the measured junction lengths for the four series of molecules. In individual conductance traces, the length of the plateaus at the molecule-dependent conductance value corresponds to the distance a junction can be elongated before it is broken. We determine the average distance a single-molecule junction can be elongated before the junction breaks by analyzing 2-dimensional conductance histograms (Figure S1-S4, details in SI part I). Considering that the Au electrodes snap back after the Au point contact is ruptured by about 6-8 Å, these elongation lengths yield the junction length and can be compared to the calculated Au-Au distance for each system.<sup>52-53</sup> We do not include the **221(Si6)** because the molecular junction breaks before it reaches the fully

elongated junction, therefore its length is not directly comparable with others.

We see that in both experiments and calculations, the **221** and **5-ring** series show a rather linear correlation between the junction length and the number of Si in the silicon arm, in agreement with past findings.<sup>52</sup> However, the **4-ring** and **222** series do not show such a linear trend. The origin of the odd-even effect in the conductance of **4-ring** series thus likely comes from an alternation of the junction length. We suggest that this mechanism might also explain the previously observed much weaker odd-even effect in linear oligogermanes.<sup>54</sup> This finding bears resemblance to the odd-even alternation effect in the conductance of self-assembled monolayers of alkanethiolates, where the results were attributed to the restricted contact angles of the molecules.<sup>55-58</sup>

The odd-even effect here is not intrinsic to the linear repeat unit that extends the functional central unit of the molecule. Instead, it is the central (bi)cyclic molecular unit that puts a structural constraint on the molecular wire as a whole. Therefore a direct comparison of the conductance of a cyclic or bicyclic molecular units cannot be done at a single length (as can be seen by comparing different columns of Table 1). By examining a series of wires this effect is eliminated and a better measure of the relative conductance of the central molecular unit is achieved. We consider this approach a general way to achieve better comparison of complex conducting and insulating molecular moieties. With this framework, we can then interrogate the roles of the different structural elements in the (bi)cyclic units.

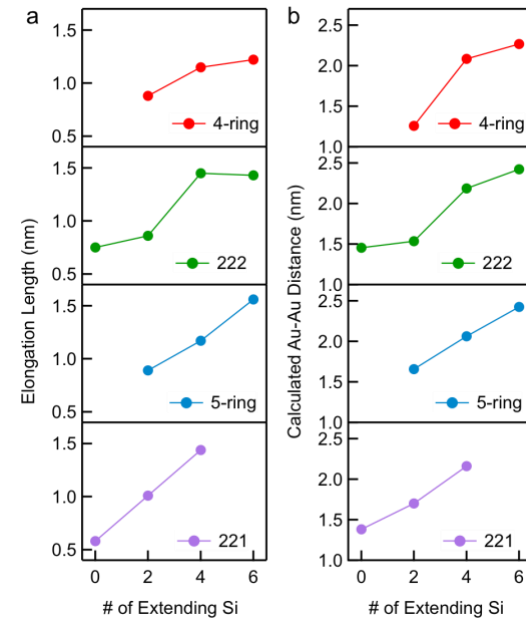


Figure 4. (a) Experimental junction elongation length and (b) Calculated Au-Au distance plotted against the molecule length for **4-ring** (red), **222** (green), **5-ring** (blue), and **221** (purple) based oligosilanes.

## The Role of Multiple Paths

When the interatomic transmission pathways are plotted for these molecules (see Figure 3, 5 and S10) a universal and striking feature is that the current is dominated by a single arm of the (bi)cyclic structures. In some cases, there are multiple pathways in the sense that there are multiple through-bond and through-space interactions within the arm (see for example **222** in Figure 5c), but we do not see this replicated across the multiple arms of

the (bi)cyclic structure. The transmission through **222** displays a through-space ring-current inside the bicyclic unit where the dihedral angles are constrained to below  $20^\circ$ . In contrast, the transmission through **221** (Figure 5d) is dominated by the single through-bond path through the bicyclic unit that is in the optimal dihedral angle configuration  $\sim 180^\circ$ . These results suggest that cyclic and bicyclic silanes do not act as fully conjugated cyclic systems where all through-bond paths in the molecule contribute to the transmission, as we know from  $\pi$ -conjugated systems such as benzene<sup>21</sup>, paracyclophanes<sup>59</sup> and larger polyaromatic molecules.<sup>60-61</sup> Instead, these cyclic and bicyclic silanes can be considered as a linear wire where the dominant silicon bridge is being conformationally constrained within the (bi)cyclic structure. Consequently, the conformation and conformational flexibility along these single paths becomes the determining factor in the transport properties for the system.

At this point, we should note that our results are not in full agreement with prior theoretical results where Löfås et al. reported that multiple paths were seen to be active through a bicyclo [2.2.2]octasilane structure similar to **222**.<sup>14</sup> In that case a TMS contact group was used where Si bonds directly to Au. It is unclear how the contact group affects the coupling through the arms in the molecule and how this may affect the appearance of destructive quantum interference in silanes. It is, however, clear that the methylthiomethyl linkers used here provides a very well-defined contact geometry where the transport properties of the  $\sigma$ -conjugated silicon structure can be systematically probed both experimentally and theoretically.<sup>10, 23, 49, 62</sup>

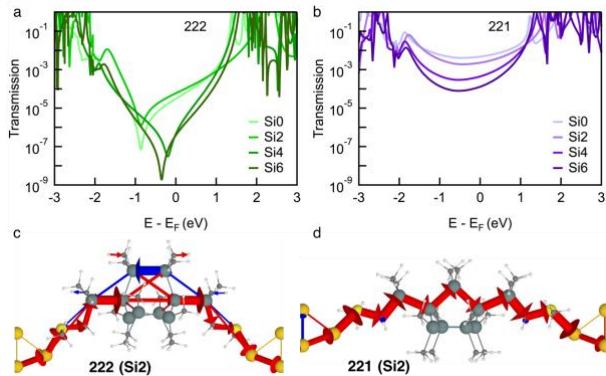


Figure 5. Calculated transmissions plotted on a semi logarithmic scale against energy for (a) **222** and (b) **221** in one of its three conformations (data for others conformations in SI). Interatomic transmission pathway analysis of (c) **222(Si2)** and (d) **221(Si2)**.

### The Role of Dihedral Angles

We can now compare the conductance of these ring systems with linear silanes. In order to do this, we first consider the shortest path in each ring. **4-ring**, **5-ring** and **221** all have three silicon atoms in the shortest path while **222** has four. Since we have measured these cyclic systems with silicon arms that have 0, 2, 4 and 6 atoms, we can consider the ratio of conductance of the shortest wires embedded in the cycle to that of their linear counterparts. Specifically, we take the measured conductance of the **4-ring**, **5-ring** and **221** wires and divide these by the conductance of linear silanes with 3, 5, 7 or 9 atoms. For the **222** wires, we divide the conductance by that of linear silanes with 4, 6, 8 or 10 silicon atoms. We list the relative zero-length conductance in Table 1 in the  $G_{n=0}/G_L$  column. While it is clear

that the conductance of the entire **221** series is very close to linear silanes of the same length, **4-ring** and **5-ring** are somewhat suppressed and **222** is significantly suppressed.

For linear silanes, it was previously shown by George et al.<sup>20</sup> that the transmission is suppressed when a dihedral angle of the silane backbone is decreased from  $180^\circ$  towards  $0^\circ$ . As we have previously explored experimentally, unconstrained linear silanes are indeed highly conducting molecular wires in their *all-transoid* conformation.<sup>10</sup> To explore the equivalence of (bi)cyclic and linear silanes, we calculate the transmission for a constrained linear permethylated hexasilane and resolve its transmission pathways in Figure 6. It is clear that decreasing the central Si-Si-Si dihedral angle from  $180^\circ$  to  $100^\circ$  only leads to a small decrease in the transmission. However, as the dihedral angle is further decreased to  $15^\circ$  an antiresonance close to the Fermi energy appears, and consequently the transmission is effectively suppressed.

We recently showed that the mechanism for this comprehensive conductance suppression in **222** is destructive quantum interference in the  $\sigma$ -system,<sup>23</sup> akin to that found in  $\pi$ -systems.<sup>63-66</sup> While all members of the **222** series have an antiresonance close to the Fermi energy as shown in Figure 5a, there are no signs of destructive interference in the transmissions of the **221** series shown in Figure 5b. Structurally very similar systems, both the **222** and **221** bicyclic units are in rigidly locked conformations. However, while all three bridges in **222** are locked into the conductance suppressing cisoid conformation, one bridge in **221** is locked into an *anti* conformation, which allows for optimal  $\sigma$ -conjugation in silane wires.

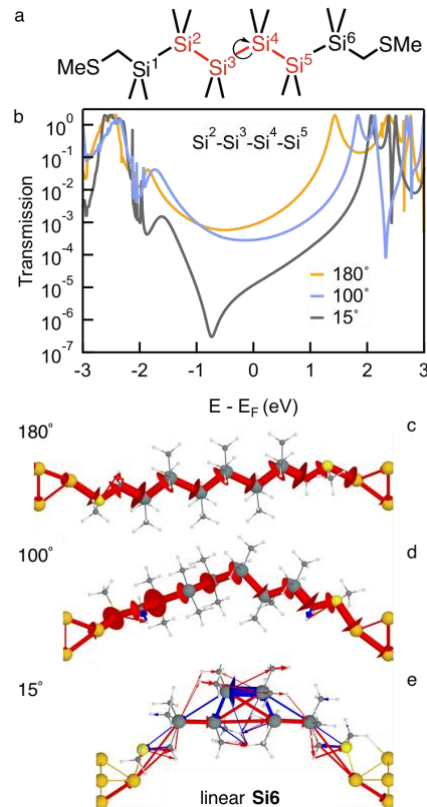


Figure 6. (a) Molecular structure of linear **Si6** indicating the central dihedral angle that is being changed in the calculations. (b) Transmissions and (c)-(e) interatomic transmission pathways of linear **Si6** constrained into a central Si-Si-Si-Si dihedral angle of  $180^\circ$ ,  $100^\circ$ , and  $15^\circ$ . The molecule is optimized to its transoid

conformation and the central dihedral angle is then manipulated without further optimization.

Beyond the magnitude of the conductance/transmission we can see that the transmission pathways for the constrained linear system closely resemble those of the two bicyclic systems in equivalent conformations: Comparing Figure 6c with Figure 5d, we see that the path of the transmission is largely the same for **221(Si2)** as for the 180° linear system. Likewise, comparing Figure 6e with Figure 5c we see that **222(Si2)** closely resembles the equivalent linear system in a 15° conformation.

Somewhat surprisingly, this behavior is largely preserved even in **4-ring** despite its smaller Si-Si-Si bond angles within the cyclic system. As plotted in Figure 3, the transmission mainly follows one through-bond path, equivalently to what is seen in Figure 6d for the linear silane constrained into a 100° dihedral angle. In **4-ring** there are also minor ring currents and through-space contributions due to the bulky TMS substituents. Still the analogy to a constrained linear system holds as the ring system is dominated by a single linear path through the molecule.

Our calculations confirm that **221** has higher conductance than **4-ring** and **5-ring** because the dihedral angles involving the three-Si path of the ring are rigidly locked in the anti-configuration (Si-Si-Si-Si = 180°±2°) providing optimal  $\sigma$ -conjugation and making it favorable for transport.<sup>17, 20, 26</sup> From the perspective of dihedral angles we may have expected **5-ring** to be the better conductor compared to **4-ring**, however, the opposite is true. While **5-ring** has conformations with well-conducting paths through the ring where dihedral angles are no lower than 125°, it also has vast conformational freedom and the less conducting conformations are likely to dominate, detailed in SI part III and previous work.<sup>12</sup> Consequently, **5-ring** has a lower measured conductance, underlining the importance of conformational freedom. The transmissions in Figure 2d of **5-ring** is for a series of conformations where the dihedral angles along the shortest path are less favorable for transport than **4-ring** for which the lowest dihedral angle is ~110°. The experimental conductance and calculated transmission of the **222** series is by far the lowest of the series examined here. With Si-Si-Si-Si dihedral angles locked in a cisoid configuration around 15-20° across the **222** bicyclic unit the suggested structure-function relationship is underlined.<sup>17, 20, 25-26</sup>

## Destructive Quantum Interference and Exponential Decay

The experimental conductance and the calculated transmission of the **222** series are low and do not show a clear exponential decay. Shown in Figure 5a, the transmission for all four members of the **222** series have sharp antiresonances in the transmission within 1 eV of the Fermi energy. The fact that there is an antiresonance close to the Fermi energy is responsible for the lack of exponential decay we see in both the experimental and theoretical results. It is also clear that the precise energetic position of the antiresonance will significantly impact the transmission at the Fermi energy.

The antiresonances are affected by the energy level alignment, which we know to be inaccurate within DFT.<sup>50-51, 67</sup> In Figure S12 we briefly examine the method dependence by calculating the transmission of the **222** series with the same DFT method using different basis sets. While such a relatively small change of methodology does not result in much qualitative change to the transmission, it is clear that the antiresonances move. Thus the antiresonance energies from DFT calculations cannot be used quantitatively.<sup>51</sup> This is responsible for the clear quantitative and qualitative disagreement between experiment and theory for the conductance trends of the **222** series seen in Figure 2e and 2f. Consequently, the transmission at the Fermi energy is

overestimated for **222(Si2)** where the antiresonance is far from the Fermi energy and underestimated for **222(Si4)** and **222(Si6)** where the antiresonance is almost right at the Fermi energy. Furthermore, in making a direct comparison between experiment and theory, it should be noted that a small bias window is applied in the experiment but not included in the calculations. This small bias window may or may not contain the antiresonance in the transmission, and could therefore affect the measured conductance.

We note that Figures S10 and S11 show that the **4-ring** and **5-ring** series also have interference features in the transmission. In both cases this feature is 0.5-1eV above the Fermi energy and does not seem to notably affect the transmission at the Fermi energy, and therefore the exponential decay of the transmission with increasing length is preserved. It remains for future work to elucidate how the structure of these cyclic systems controls interference effects in saturated molecules.

## CONCLUSIONS

By measuring the single-molecule conductance of four series of functionalized cyclic and bicyclic permethylated silane wires, we establish the previously suggested structure-function relationship for the conductance of silane wires. Through DFT calculations we show that unlike cyclic  $\pi$ -conjugated molecules, the transmission through cyclic and bicyclic  $\sigma$ -conjugated molecules is dominated by a single path through the molecule. In agreement with the dihedral angle dependence of  $\sigma$ -conjugation, we establish the conductance relationship as  $G_{221} > G_{4\text{-ring}} > G_{5\text{-ring}} > G_{222}$ . This suggests that the conductive properties of cyclic and bicyclic silanes largely can be understood by considering them as constrained linear systems. The structurally similar bicyclic series **221** and **222** underline this difference; the former a fully  $\sigma$ -conjugated system with high conductance, the latter a case of conductance suppression due to destructive  $\sigma$ -interference.

By measuring the conductance of a series of linearly extended (bi)cyclic molecules, we reveal a general method that takes the structural variation of the wires into account. The conducting properties of the central molecular unit can be isolated as the exponential decay constants of the series do not differ significantly, thus confirming that the Si—Si  $\sigma$ -conjugation in the extending linear backbones is not notably affected by the ring. We find this is a reliable and general way to determine the conductance of silicon rings. We find it noteworthy that this approach can eliminate the effect of structural variation and may be a general approach for single-molecule studies of complex molecular structures.

## ASSOCIATED CONTENT

### Supporting Information

The Supporting Information is available free of charge on the ACS Publications website at DOI:  
Additional Figures, STM-BJ experimental details, DFT calculation details, and characterization data (PDF)

## AUTHOR INFORMATION

### Corresponding Author

\*xiaoxs@shnu.edu.cn  
\*gsolomon@chem.ku.dk  
\*lv2117@columbia.edu

### Present Addresses

H.L.: Department of Chemistry, Columbia University, New York, NY 10027, United States

Z.S.: School of Chemistry and Chemical Engineering, Shanghai Jiao Tong University, Shanghai 200240, China

T.A.S.: Department of Chemistry, University of California, Berkeley, Berkeley, CA 94720, United States

## Author Contributions

‡H.L., M.H.G. and Z.S. contributed equally.

## Notes

The authors declare no competing financial interests.

## ACKNOWLEDGMENT

We thank the NSF for the support of experimental studies under grant no. CHE-1404922 and CHE-1764256 (H.L. and M.N.). G.C.S. and M.H.G. received funding from the Danish Council for Independent Research|Natural Sciences. Z.S., Y.C., Q.Z., T.L., and S. X. are sponsored by National Natural Science Foundation of China (No. 21473113, 51502173, 21772123), Program of Shanghai Academic/Technology Research Leader (No. 16XD1402700), Program for Professor of Special Appointment (Eastern Scholar) at Shanghai Institutions of Higher Learning (No. 2013-57), “Shuguang Program” supported by Shanghai Education Development Foundation and Shanghai Municipal Education Commission (14SG40), Program for Changjiang Scholars, Innovative Research Team in University (IRT1269), and International Joint Laboratory on Resource Chemistry (IJLRC). T.A.S. was supported by the NSF Graduate Research Fellowship under grant no. 11-44155.

## REFERENCES

1. Ieong, M.; Doris, B.; Kedzierski, J.; Rim, K.; Yang, M., Silicon Device Scaling to the Sub-10-nm Regime. *Science* **2004**, *306* (5704), 2057-2060.
2. Wallner, A.; Emanuelsson, R.; Baumgartner, J.; Marschner, C.; Ottosson, H., Coupling of Disilane and Trisilane Segments Through Zero, One, Two, and Three Disilanyl Bridges in Cyclic and Bicyclic Saturated Carbosilanes. *Organometallics* **2013**, *32* (2), 396-405.
3. Fischer, R.; Frank, D.; Gaderbauer, W.; Kayser, C.; Mechtler, C.; Baumgartner, J.; Marschner, C.,  $\alpha,\omega$ -Oligosilyl Dianions and Their Application in the Synthesis of Homo- and Heterocyclosilanes. *Organometallics* **2003**, *22* (18), 3723-3731.
4. Wallner, A.; Hlina, J.; Konopa, T.; Wagner, H.; Baumgartner, J.; Marschner, C.; Flörke, U., Cyclic and Bicyclic Methylpolysilanes and Some Oligosilanylene-Bridged Derivatives. *Organometallics* **2010**, *29* (12), 2660-2675.
5. Wagner, H.; Baumgartner, J.; Marschner, C.; Poelt, P., Rearrangement/Fragmentation Reactions of Oligosilanes with Aluminum Chloride. *Organometallics* **2011**, *30* (15), 3939-3954.
6. Tsurasaki, A.; Koyama, Y.; Kyushin, S., Decasilahexahydrotriquinacene and Decasilaisotwistane:  $\sigma$  Conjugation on a Bowl Surface. *J. Am. Chem. Soc.* **2017**, *139* (11), 3982-3985.
7. Li, Y.; Li, J.; Zhang, J.; Song, H.; Cui, C., Isolation of R6Si6 Dianion: A Bridged Tricyclic Isomer of Dianionic Hexasilabenzene. *J. Am. Chem. Soc.* **2018**, *140* (4), 1219-1222.
8. Press, E. M.; Marro, E. A.; Surampudi, S. K.; Siegler, M. A.; Tang, J. A.; Klausen, R. S., Synthesis of a Fragment of Crystalline Silicon: Poly(Cyclosilane). *Angew. Chem. Int. Ed.* **2017**, *56* (2), 568-572.
9. Marro, E. A.; Press, E. M.; Siegler, M. A.; Klausen, R. S., Directional Building Blocks Determine Linear and Cyclic Silicon Architectures. *J. Am. Chem. Soc.* **2018**, *140* (18), 5976-5986.
10. Su, T. A.; Li, H.; Steigerwald, M. L.; Venkataraman, L.; Nuckolls, C., Stereoelectronic switching in single-molecule junctions. *Nat. Chem.* **2015**, *7* (3), 215-220.
11. Li, H.; Garner, M. H.; Su, T. A.; Jensen, A.; Inkpen, M. S.; Steigerwald, M. L.; Venkataraman, L.; Solomon, G. C.; Nuckolls, C., Extreme Conductance Suppression in Molecular Siloxanes. *J. Am. Chem. Soc.* **2017**, *139* (30), 10212-10215.
12. Li, H.; Garner, M. H.; Shangguan, Z.; Zheng, Q.; Su, T. A.; Neupane, M.; Li, P.; Velian, A.; Steigerwald, M. L.; Xiao, S.; Nuckolls, C.; Solomon, G. C.; Venkataraman, L., Conformations of cyclopentasilane stereoisomers control molecular junction conductance. *Chem. Sci.* **2016**, *7* (9), 5657-5662.
13. Magoga, M.; Joachim, C., Conductance of molecular wires connected or bonded in parallel. *Phys. Rev. B* **1999**, *59* (24), 16011-16021.
14. Löfås, H.; Emanuelsson, R.; Ahuja, R.; Grigoriev, A.; Ottosson, H., Conductance through Carbosilane Cage Compounds: A Computational Investigation. *J. Phys. Chem. C* **2013**, *117* (42), 21692-21699.
15. Emanuelsson, R.; Löfås, H.; Wallner, A.; Nauroozi, D.; Baumgartner, J.; Marschner, C.; Ahuja, R.; Ott, S.; Grigoriev, A.; Ottosson, H., Configuration- and Conformation-Dependent Electronic-Structure Variations in 1,4-Disubstituted Cyclohexanes Enabled by a Carbon-to-Silicon Exchange. *Chem. - Eur. J.* **2014**, *20* (30), 9304-9311.
16. Tsuji, H.; Michl, J.; Tamao, K., Recent experimental and theoretical aspects of the conformational dependence of UV absorption of short chain peralkylated oligosilanes. *J. Organomet. Chem.* **2003**, *685* (1), 9-14.
17. Bande, A.; Michl, J., Conformational Dependence of  $\sigma$ -Electron Delocalization in Linear Chains: Permethylated Oligosilanes. *Chem. - Eur. J.* **2009**, *15* (34), 8504-8517.
18. Jovanovic, M.; Antic, D.; Rooklin, D.; Bande, A.; Michl, J., Intuitive Understanding of  $\sigma$  Delocalization in Loose and  $\sigma$  Localization in Tight Helical Conformations of an Oligosilane Chain. *Chemistry – An Asian Journal* **2017**, *12* (11), 1250-1263.
19. Jovanovic, M.; Michl, J., Understanding the Effect of Conformation on Hole Delocalization in Poly(dimethylsilane). *J. Am. Chem. Soc.* **2018**, *140* (36), 11158-11160.
20. George, C. B.; Ratner, M. A.; Lambert, J. B., Strong Conductance Variation in Conformationally Constrained Oligosilane Tunnel Junctions†. *J. Phys. Chem. A* **2009**, *113* (16), 3876-3880.
21. Solomon, G. C.; Herrmann, C.; Hansen, T.; Mujica, V.; Ratner, M. A., Exploring local currents in molecular junctions. *Nat. Chem.* **2010**, *2* (3), 223-228.
22. Li, C.; Pobelov, I.; Wandlowski, T.; Bagrets, A.; Arnold, A.; Evers, F., Charge Transport in Single Au | Alkanedithiol | Au Junctions: Coordination Geometries and Conformational Degrees of Freedom. *J. Am. Chem. Soc.* **2008**, *130* (1), 318-326.
23. Garner, M. H.; Li, H.; Chen, Y.; Su, T. A.; Shangguan, Z.; Paley, D. W.; Liu, T.; Ng, F.; Li, H.; Xiao, S.; Nuckolls, C.; Venkataraman, L.; Solomon, G. C., Comprehensive suppression of single-molecule conductance using destructive  $\sigma$ -interference. *Nature* **2018**, *558* (7710), 415-419.
24. Michl, J.; West, R., Conformations of Linear Chains. Systematics and Suggestions for Nomenclature. *Acc. Chem. Res.* **2000**, *33* (12), 821-823.
25. Tsuji, H.; Terada, M.; Toshimitsu, A.; Tamao, K.,  $\sigma\sigma^*$  Transition in anti,cisoid Alternating Oligosilanes: Clear-Cut Evidence for Suppression of Conjugation Effect by a cisoid Turn. *J. Am. Chem. Soc.* **2003**, *125* (25), 7486-7487.
26. Fukazawa, A.; Tsuji, H.; Tamao, K., all-anti-Octasilane: Conformation Control of Silicon Chains Using the Bicyclic Trisilane as a Building Block. *J. Am. Chem. Soc.* **2006**, *128* (21), 6800-6801.
27. Tsuji, H.; Fogarty, H. A.; Ehara, M.; Fukuda, R.; Casher, D. L.; Tamao, K.; Nakatsuji, H.; Michl, J., Electronic Transitions in Conformationally Controlled Tetrasilanes with a Wide Range of SiSiSiSi Dihedral Angles. *Chem. - Eur. J.* **2014**, *20* (30), 9431-9441.
28. Kanazawa, Y.; Tsuji, H.; Ehara, M.; Fukuda, R.; Casher, D. L.; Tamao, K.; Nakatsuji, H.; Michl, J., Electronic Transitions in Conformationally Controlled Peralkylated Hexasilanes. *ChemPhysChem* **2016**, *17* (19), 3010-3022.
29. van der Laan, G. P.; de Haas, M. P.; Hummel, A.; Frey, H.; Möller, M., Charge Carrier Mobilities in Substituted Polysilylenes: Influence of Backbone Conformation. *The Journal of Physical Chemistry* **1996**, *100* (13), 5470-5480.
30. Grozema, F. C.; Siebbeles, L. D. A.; Warman, J. M.; Seki, S.; Tagawa, S.; Scherf, U., Hole Conduction along Molecular Wires:  $\sigma$ -Bonded Silicon Versus  $\pi$ -Bond-Conjugated Carbon. *Advanced Materials* **2002**, *14* (3), 228-231.
31. Kitao, T.; Bracco, S.; Comotti, A.; Sozzani, P.; Naito, M.; Seki, S.; Uemura, T.; Kitagawa, S., Confinement of Single Polysilane Chains in Coordination Nanospaces. *J. Am. Chem. Soc.* **2015**, *137* (15), 5231-5238.
32. Huang, M.-J.; Hsu, L.-Y.; Fu, M.-D.; Chuang, S.-T.; Tien, F.-W.; Chen, C.-h., Conductance of Tailored Molecular Segments: A Rudimentary Assessment by Landauer Formulation. *J. Am. Chem. Soc.* **2014**, *136* (5), 1832-1841.

33. Hsu, L.-Y.; Rabitz, H., Theory of molecular conductance using a modular approach. *J. Chem. Phys.* **2016**, *145* (23), 234702.

34. Klausen, R. S.; Widawsky, J. R.; Steigerwald, M. L.; Venkataraman, L.; Nuckolls, C., Conductive molecular silicon. *J Am Chem Soc* **2012**, *134* (10), 4541-4.

35. Marschner, C., Preparation and Reactions of Polysilanyl Anions and Dianions. *Organometallics* **2006**, *25* (9), 2110-2125.

36. Fischer, R.; Baumgartner, J.; Kickelbick, G.; Marschner, C., The First Stable  $\beta$ -Fluorosilylanion. *Journal of the American Chemical Society* **2003**, *125* (12), 3414-3415.

37. Ogura, K.; Fujita, M.; Takahashi, K.; Iida, H., An improved procedure for efficient generation of methyl(or p-tolyl)thiomethyl Grignard reagent and its use in organic syntheses. *Chemistry Letters* **1982**, (11), 1697-1698.

38. Iwamoto, T.; Tsushima, D.; Kwon, E.; Ishida, S.; Isobe, H., Persilastaffanes: Design, Synthesis, Structure, and Conjugation between Silicon Cages. *Angewandte Chemie International Edition* **2012**, *51* (10), 2340-2344.

39. Xu, B.; Tao, N. J., Measurement of Single-Molecule Resistance by Repeated Formation of Molecular Junctions. *Science* **2003**, *301* (5637), 1221-1223.

40. Venkataraman, L.; Klare, J. E.; Tam, I. W.; Nuckolls, C.; Hybertsen, M. S.; Steigerwald, M. L., Single-Molecule Circuits with Well-Defined Molecular Conductance. *Nano Lett.* **2006**, *6* (3), 458-462.

41. Perdew, J. P.; Burke, K.; Ernzerhof, M., Generalized Gradient Approximation Made Simple. *Phys. Rev. Lett.* **1996**, *77* (18), 3865-3868.

42. Mortensen, J. J.; Hansen, L. B.; Jacobsen, K. W., Real-space grid implementation of the projector augmented wave method. *Phys. Rev. B* **2005**, *71* (3), 035109.

43. Larsen, A. H.; Vanin, M.; Mortensen, J. J.; Thygesen, K. S.; Jacobsen, K. W., Localized atomic basis set in the projector augmented wave method. *Phys. Rev. B* **2009**, *80* (19), 195112.

44. Larsen, A. H.; Mortensen, J. J.; Blomqvist, J.; E. Castelli, I.; Christensen, R.; Dulak, M.; Friis, J.; N. Groves, M.; Hammer, B.; Hargus, C.; D. Hermes, E.; C. Jennings, P.; Jensen, P. B.; Kermode, J.; R. Kitchin, J.; Kolsbjerg, E. L.; Kubal, J.; Kaasbjerg, K.; Lysgaard, S.; Maronsson, J. B.; Maxson, T.; Olsen, T.; Pastewka, L.; Peterson, A.; Rostgaard, C.; Schiøtz, J.; Schütt, O.; Strange, M.; S. Thygesen, K.; Vegge, T.; Vilhelmsen, L.; Walter, M.; Zeng, Z.; W. Jacobsen, K., The atomic simulation environment—a Python library for working with atoms. *J. Phys.: Condens. Matter* **2017**, *29* (27), 273002.

45. M. Soler, J.; Artacho, E.; D. Gale, J.; García, A.; Junquera, J.; Ordejón, P.; Sánchez-Portal, D., The SIESTA method for ab initio order-N materials simulation. *J. Phys.: Condens. Matter* **2002**, *14* (11), 2745.

46. Brandbyge, M.; Mozos, J.-L.; Ordejón, P.; Taylor, J.; Stokbro, K., Density-functional method for nonequilibrium electron transport. *Phys. Rev. B* **2002**, *65* (16), 165401.

47. Atomistix ToolKit version2016.3 (QuantumWiseA/S,2016); quantumwise.com.

48. Virtual NanoLab version2016.3 (QuantumWiseA/S,2016); quantumwise.com.

49. Pramanik, A.; Sarkar, P., Understanding the conductance switching of permethyloligosilanes: A theoretical approach. *J. Chem. Phys.* **2015**, *143* (11), 114314.

50. Tamlyn, I.; Darancet, P.; Quek, S. Y.; Bonev, S. A.; Neaton, J. B., Electronic energy level alignment at metal-molecule interfaces with a GW approach. *Phys. Rev. B* **2011**, *84* (20).

51. Pedersen, K. G. L.; Strange, M.; Leijnse, M.; Hedegård, P.; Solomon, G. C.; Paaske, J., Quantum interference in off-resonant transport through single molecules. *Phys. Rev. B* **2014**, *90* (12), 125413.

52. Kamenetska, M.; Koentopp, M.; Whalley, A. C.; Park, Y. S.; Steigerwald, M. L.; Nuckolls, C.; Hybertsen, M. S.; Venkataraman, L., Formation and Evolution of Single-Molecule Junctions. *Phys. Rev. Lett.* **2009**, *102* (12), 126803.

53. Yanson, A. I.; Bollinger, G. R.; van den Brom, H. E.; Agrait, N.; van Ruitenbeek, J. M., Formation and manipulation of a metallic wire of single gold atoms. *Nature* **1998**, *395* (6704), 783-785.

54. Su, T. A.; Li, H.; Zhang, V.; Neupane, M.; Batra, A.; Klausen, R. S.; Kumar, B.; Steigerwald, M. L.; Venkataraman, L.; Nuckolls, C., Single-Molecule Conductance in Atomically Precise Germanium Wires. *J. Am. Chem. Soc.* **2015**, *137* (38), 12400-12405.

55. Frederiksen, T.; Munuera, C.; Ocal, C.; Brandbyge, M.; Paulsson, M.; Sanchez-Portal, D.; Arnau, A., Exploring the Tilt-Angle Dependence of Electron Tunneling across Molecular Junctions of Self-Assembled Alkanethiols. *ACS Nano* **2009**, *3* (8), 2073-2080.

56. Thuo, M. M.; Reus, W. F.; Nijhuis, C. A.; Barber, J. R.; Kim, C.; Schulz, M. D.; Whitesides, G. M., Odd-Even Effects in Charge Transport across Self-Assembled Monolayers. *J. Am. Chem. Soc.* **2011**, *133* (9), 2962-2975.

57. Jiang, L.; Sangeeth, C. S. S.; Nijhuis, C. A., The Origin of the Odd-Even Effect in the Tunneling Rates across EGaIn Junctions with Self-Assembled Monolayers (SAMs) of n-Alkanethiols. *J. Am. Chem. Soc.* **2015**, *137* (33), 10659-10667.

58. Yuan, L.; Thompson, D.; Cao, L.; Nerngchangnong, N.; Nijhuis, C. A., One Carbon Matters: The Origin and Reversal of Odd-Even Effects in Molecular Diodes with Self-Assembled Monolayers of Ferrocenyl-Alkanethiols. *J. Phys. Chem. C* **2015**, *119* (31), 17910-17919.

59. Vazquez, H.; Skouta, R.; Schneebeli, S.; Kamenetska, M.; Breslow, R.; Venkataraman, L.; Hybertsen, M. S., Probing the conductance superposition law in single-molecule circuits with parallel paths. *Nat. Nanotechnol.* **2012**, *7* (10), 663-667.

60. Stuyver, T.; Blotwijk, N.; Fias, S.; Geerlings, P.; De Proft, F., Exploring Electrical Currents through Nanographenes: Visualization and Tuning of the through-Bond Transmission Paths. *ChemPhysChem* **2017**, *18* (21), 3012-3022.

61. Nozaki, D.; Toher, C., Is the Antiresonance in Meta-Contacted Benzene Due to the Destructive Superposition of Waves Traveling Two Different Routes around the Benzene Ring? *J. Phys. Chem. C* **2017**, *121* (21), 11739-11746.

62. Wang, M.; Wang, Y.; Sanvito, S.; Hou, S., The low-bias conducting mechanism of single-molecule junctions constructed with methylsulfide linker groups and gold electrodes. *J. Chem. Phys.* **2017**, *147* (5), 054702.

63. Sautet, P.; Joachim, C., Electronic interference produced by a benzene embedded in a polyacetylene chain. *Chemical Physics Letters* **1988**, *153* (6), 511-516.

64. Mayor, M.; Weber, H. B.; Reichert, J.; Elbing, M.; von Hänisch, C.; Beckmann, D.; Fischer, M., Electric Current through a Molecular Rod—Relevance of the Position of the Anchor Groups. *Angew. Chem. Int. Ed.* **2003**, *42* (47), 5834-5838.

65. Guédon, C. M.; Valkenier, H.; Markussen, T.; Thygesen, K. S.; Hummelen, J. C.; van der Molen, S. J., Observation of quantum interference in molecular charge transport. *Nature Nanotechnology* **2012**, *7*, 305.

66. Arroyo, C. R.; Tarkuc, S.; Frisenda, R.; Seldenthuis, J. S.; Woerde, C. H. M.; Eelkema, R.; Grozema, F. C.; van der Zant, H. S. J., Signatures of Quantum Interference Effects on Charge Transport Through a Single Benzene Ring. *Angew. Chem. Int. Ed.* **2013**, *52* (11), 3152-3155.

67. Strange, M.; Thygesen, K. S., Towards quantitative accuracy in first-principles transport calculations: The GW method applied to alkane/gold junctions. *Beilstein Journal of Nanotechnology* **2011**, *2*, 746-754.

Insert Table of Contents artwork here

